JOINT INSTITUTE FOR NUCLEAR RESEARCH

FINAL REPORT ON THE INTEREST PROGRAMME

“Radiation protection and the safety of radiation sources.”

Supervisor:
Dr. Said AbouElazm

Student:
Elizabeth Vega
Center of Technological Applications and Nuclear Development (CEADEN)

Participation period:
November 5 – December 14, Wave 11

Dubna, 2024

Abstract

This work investigates the relationship between the energy resolution of various detectors (BGO, NaI, and CdTe) and the applied voltage, using radioactive sources such as Co60 and Cs137. For the BGO detector, voltage variations from 1200V to 2000V were examined, revealing that for values above 1600V, the energy resolution improved by approximately 27.67% at 1173 keV. In contrast, the NaI detector, tested with voltage ranges from 900V to 1300V, showed good resolution values that enhanced with increased voltage, achieving resolutions below 5% at 1173 keV for voltages over 1100V. The energy calibration for BGO and NaI detectors was performed, yielding the calibration equations $E(keV)=102.72734\times Ch-4.94908$ for BGO and $E(keV)=105.23113\times Ch-153.00768$ for NaI.

Additionally, the resolution and energy calibration of the X-123CdTe detector were determined, with a resolution of 1.27% at 122 keV and a calibration curve equation of $E(keV)=1.70369\times Ch-452.07993$. Furthermore, the mass attenuation coefficients of aluminum (Al) and copper (Cu) were found to be 0.2913 cm^2/g and 1.666 cm^2/g, respectively, with relative errors less than 5% compared to tabulated values. These results underline the significance of optimizing detector performance for various applications in radiation protection and imaging.

Introduction

Bismuth germanate (BGO) detectors, for instance, are extensively utilized due to their high efficiency and stopping power for gamma-ray detection. These detectors have proven their versatility and effectiveness in medical and nuclear physics applications. In positron emission tomography (PET), BGO detectors coupled with photodiodes significantly improve spatial resolution [1]. Moreover, BGO active shields enhance the sensitivity of high-purity germanium detectors by suppressing background radiation [2]. Comparative studies through Monte Carlo simulations indicate that BGO detectors, although boasting superior efficiency, present lower resolution compared to NaI(Tl) detectors [3]. Understanding the interplay between detector resolution and applied voltage is crucial for optimizing particle detection and imaging systems, leading to the objective of determining this relationship for BGO detectors.

Sodium iodide (NaI) detectors also play a crucial role in gamma-ray detection due to their high efficiency and excellent energy resolution. Large NaI detectors can achieve outstanding energy resolution, as evidenced by a system demonstrating 1.6% resolution at 22.6 MeV [4]. These detectors are well-suited for in-situ measurements of 137Cs in alpine environments [5]. The development of CMOS-coupled NaI scintillation detectors has further improved the linearity across a wide range of activity levels, demonstrating similar sensitivity and noise characteristics to photomultiplier tube-based systems over short time scales [6]. Therefore, investigating the

relationship between energy resolution and applied voltage for NaI detectors is another critical objective of this work.

Additionally, the process of energy calibration is fundamental for both BGO and NaI detectors. Energy calibration involves relating the channel numbers to their corresponding energies, typically resulting in a linear function. This process requires certified radioactive sources with known energies to ensure accuracy. The calibration equation is generally expressed as:

$$E = mCh + n \quad (1)$$

where E represents the energy, m is the slope, Ch is the channel number, and n is the y-intercept. These parameters depend on the electronic pulse amplification and classification devices, the power supply of the photomultiplier, and the characteristics of the detector. The objective here is to perform the energy calibration of BGO and NaI detectors using known radioactive sources.

Furthermore, cadmium telluride (CdTe) semiconductor detectors have garnered attention for X-ray and gamma-ray detection due to their high atomic numbers and large bandgap energies, allowing them to operate at room temperature [7]. These detectors provide enhanced spatial and energetic resolution compared to traditional scintillation detectors, making them suitable for medical imaging applications, including single-photon emission computed tomography [8]. Despite their advantages, CdTe detectors face challenges such as charge loss due to low hole mobility and short carrier lifetime. Recent advancements in crystal production and electrode design have improved these detectors' spectral properties and overall performance [9]. This report aims to determine the resolution of the X-123CdTe detector and perform its energy calibration.

Finally, the attenuation of ionizing radiation is a critical topic in medical physics for both radiation protection and imaging. Computational simulations model radiation attenuation through various materials, providing essential insights into shielding requirements and dose calculations [10]. The interaction of X-rays with matter, involving processes such as coherent scattering, the photoelectric effect, Compton scattering, pair production, and photodisintegration, depends on photon energy and medium composition [11]. This report will determine the attenuation coefficients of aluminum (Al) and copper (Cu), materials commonly used in shielding certain radioactive sources.

Task 1: Determination of the relationship between the applied voltage and the resolution of a BGO detector using a Co60 radioactive source.

The performance of a BGO detector was evaluated using a Co60 radioactive source, while adjusting the applied voltage between 1200V and 2000V. To ascertain the detector's energy resolution, the following resolution formula was employed:

$$R = \frac{FWHM}{H_0} \quad (2)$$

where FWHM (Full Width at Half Maximum) represents the width of the distribution at half the peak height, and Ho is the centroid. This parameter is dimensionless and typically expressed as a percentage.

The value of FWHM was determined using the relation:

$$FWHM = 2.35 * \sigma \quad (3)$$

where σ denotes the standard deviation of the distribution.

ROOT software was use to derived the values of Ho and σ.

Results:

Table 1 shows the resolution values obtained for the BGO detector at 1173 keV, making variations in the applied voltage from 1200 V to 2000 V. In Figure 1 can be seen the relation between them. Above 1600 V, the energy resolution improves, but increasing the voltage may damage the detector.

Table 1. Applied voltage and the corresponding resolution %

Applied voltage (V)	σ	Resolution (%)
1200	0.46	68.2
1300	0.25	42.67
1400	0.29	35.07
1500	0.40	31.36
1600	0.57	30.57
1700	0.74	28.28
1900	1.22	26.73
2000	1.55	26.73

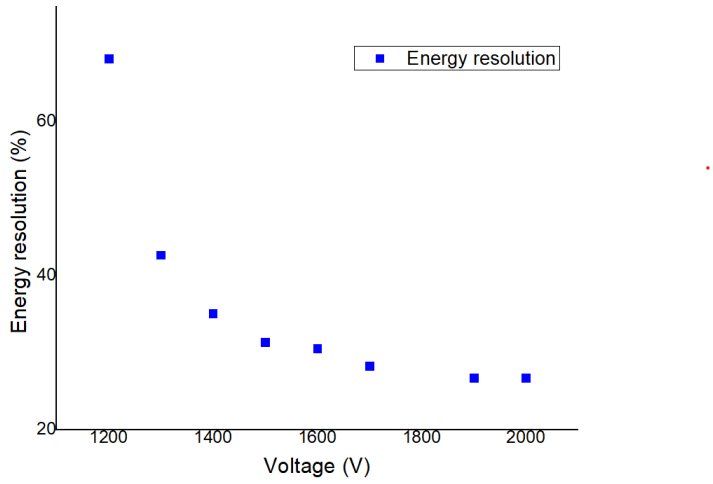

Figure 1. Relation between applied voltage and resolution %.

Task 2: Determination of the relationship between the applied voltage and the resolution of a NaI detector using a Co60 radioactive source.

Results:

As in the previous task, the response of the detector (in this case, NaI) will be determined using a Co60 radioactive source.

Table 2 shows the resolution values obtained for the NaI detector at 1173 keV, making variations in the applied voltage from 900 V to 1300 V, obtaining percentages between 4-6 %. Figure 2 shows that the energy resolution of the detector improves as the voltage is increased. Above 1100 V, the energy resolution improves, but increasing the voltage may damage the detector. Can be see that NaI detectors has better resolution than the BGO detectors.

Table 2. Applied voltage and the corresponding resolution %

Applied voltage (V)	σ	Resolution (%)
900	0.56	5.58
1000	0.92	5.32
1100	1.49	5.31
1200	2.01	4.78
1300	2.47	4.22

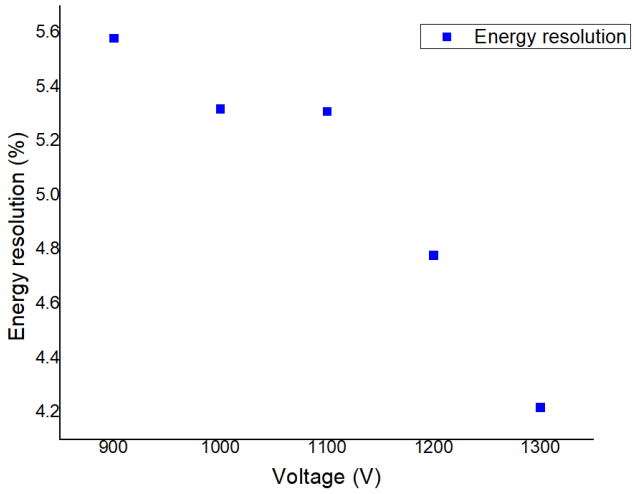

Figure 2. Relation between applied voltage and resolution %.

Task 3: Energy calibration of BGO and NaI detectors.

Knowing the energy spectrum of both sources (Cs137 and Co60) we were able to identify them in the experimental data provided. Using ROOT program we obtained the mean by making gaussian fit.

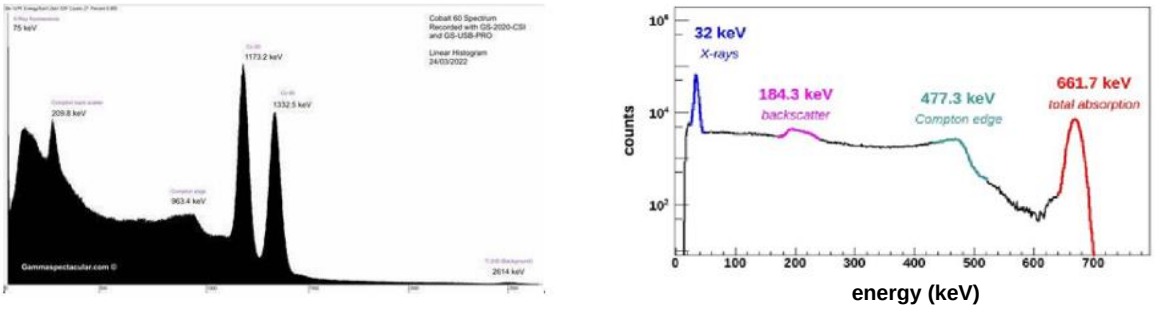

(a) (b)

Figure 3. Energy spectrum of Co60 (a) and Cs137 (b).

Results:

In the BGO detector case a linear regression was performed that resulted in the following calibration line:

$$E\ (keV) = 102.72734 * Ch - 4.94908 \quad (4)$$

Table 3. Channel number(mean) and energy of peaks for BGO detector.

Channel number	Energy (keV)
6.47	662
12.27	1253
24.38	2500

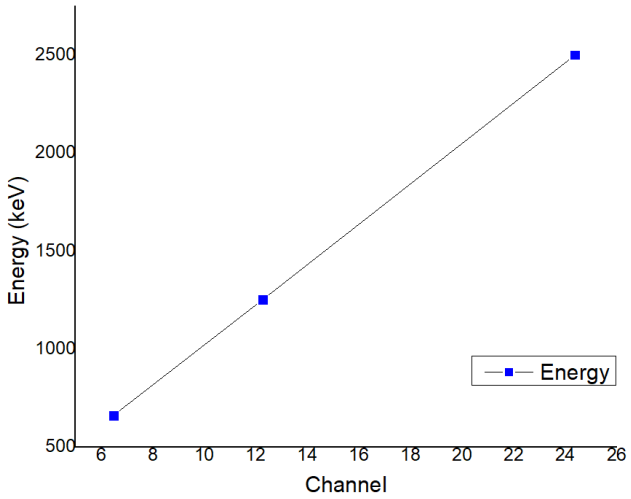

Figure 4. Calibration curve of BGO detector.

In the NaI detector case a linear regression was performed that resulted in the following calibration line:

$$E\ (keV) = 105.23113 * Ch - 153.00768 \quad (5)$$

Table 4. Channel number(mean) and energy of peaks for NaI detector.

Channel number	Energy (keV)
7.70	662

12.63	1173
14.15	1333
25.19	2500

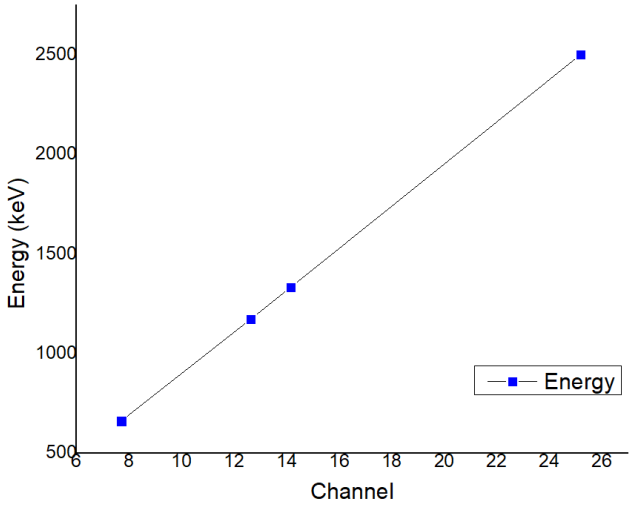

Figure 5. Calibration curve of NaI detector.

Task 3: Calibration and determination of the resolution of the X-123CdTe detector.

Results:

The source that will be used to determine the resolution of this detector is Co57. The procedure is the same as in tasks 1 and 2.

Table 5. FWHM of X-123CdTe detector with Co57.

FWHM	Resolution (%)
4.10	1.27

As in the task 3, we will used known sources to calibrate the detector. The sources that we are going to use in this case are Cs137, Co60 and Am241. And the calibration line are going to be:

$$E\ (keV) = 1.70369 * Ch - 452.07993 \quad (6)$$

Table 6. Channel number(mean) and energy of peaks for X-123CdTe detector.

Channel number	Energy (keV)
654.27	662
322.57	122

314.32	59.5

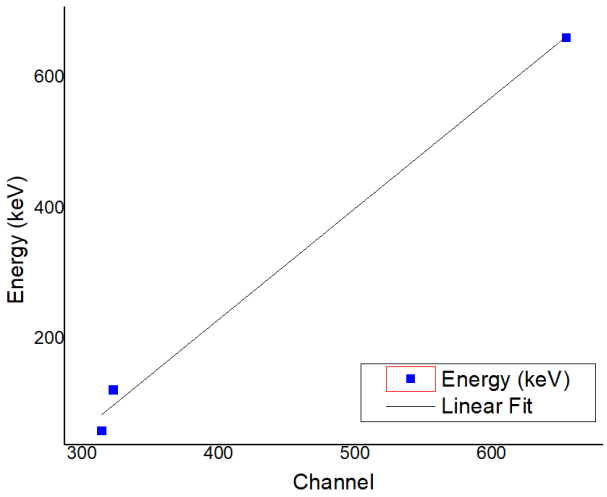

Figure 6. Calibration curve of X-123CdTe detector.

Task 4: Determination of the attenuation coefficient of Al and Cu using the X-123CdTe detector.

The X-123CdTe detector and, as the radioactive source, Am241 were used. To determine the attenuation coefficient of Al and Cu, we used the expression:

$$I = I_o e^{-\mu x} \quad (7)$$

where Io is the initial intensity of the radiation beam, I is the intensity of the radiation beam once it passes through the material, μ is the attenuation coefficient of the material and x is the thickness of the material.

Working mathematically with expression 7, we can arrive at the following relationship that corresponds to a linear fit, where the slope of the fit will be the attenuation coefficient of the material:

$$ln\frac{I_0}{I} = \mu * x \quad (8)$$

Table 7. Values used to determine the linear attenuation coefficient of Al.

X (cm)	Io	I	Io/I	Ln (Io/I)
0.052	2849	2778	-1.03	0.03
0.11	2849	2471	1.15	0.14
0.16	2849	2457	1.16	0.15
0.22	2849	2387	1.19	0.18
0.28	2849	2363	1.21	0.19
0.30	2849	2134	1.34	0.29
0.50	2849	1896	1.50	0.41

0.80	2849	1386	2.06	0.72
1.60	2849	741	3.84	1.35
2.90	2849	277	10.29	2.33
3.40	2849	213	13.38	2.59
4.37	2849	86	33.13	3.50

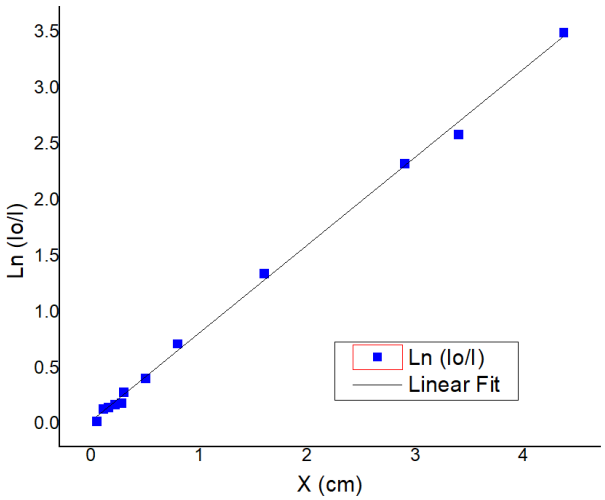

Figure 7. Attenuation curve for Al.

Table 8. Values used to determine the linear attenuation coefficient of Cu.

X (cm)	Io	I	Io/I	Ln (Io/I)
0.02	2634	2085	1.26	0.23
0.05	2634	1490	1.77	0.57
0.07	2634	1215	2.17	0.77
0.1	2634	701	3.76	1.32
0.15	2634	298	8.84	2.18
0.2	2634	160	16.46	2.80
0.25	2634	73	36.08	3.59

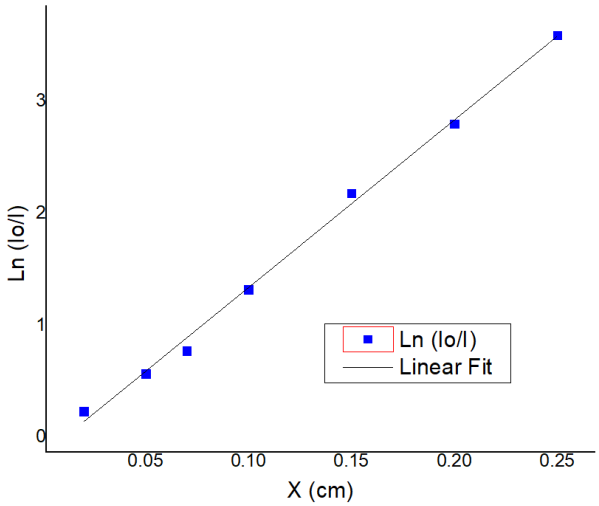

Figure 8. Attenuation curve for Cu.

Conclusion

In this work, we investigated the relationship between the energy resolution of a BGO detector and the applied voltage using a Co60 source, with voltage variations ranging from 1200V to 2000V. It was found that for voltage values above 1600V, the energy resolution of the detector improves by approximately 27.67% at 1173 keV. Similarly, the relationship between the energy resolution of a NaI detector and the applied voltage was analyzed using a Co60 source, with voltage variations ranging from 900V to 1300V. The results demonstrated good resolution values that improved with increased voltage, achieving values below 5% at 1173 keV for voltages greater than 1100V.

The energy calibration of the BGO and NaI detectors was conducted using known radiation sources, Co60 and Cs137. For the BGO detector, the calibration equation obtained was $E(keV)=102.72734\times Ch-4.94908$, where E represents the energy in keV and Ch is the channel number corresponding to the peak centroid. For the NaI detector, the calibration equation was $E(keV)=105.23113\times Ch-153.00768$.

In addition, the resolution of the X-123CdTe detector was determined using a Co57 source, resulting in a resolution of 1.27% at 122 keV. The calibration curve for this detector, performed with known sources Cs137, Co57, and Am241, was $E(keV)=1.70369\times Ch-452.07993$, where E is the energy in keV and Ch is the channel number.

Lastly, the mass attenuation coefficients of aluminum (Al) and copper (Cu) were determined to be 0.2913 cm^2/g and 1.666 cm^2/g, respectively, both with a relative error of less than 5% compared to the tabulated values for the photon energy used.

These findings highlight the importance of understanding and optimizing the energy resolution and calibration of different types of detectors, which is crucial for applications in radiation protection and imaging.

References

[1] Derenzo, S. E. (1984). Positron emission tomography: Principles and instrumentation. *Journal of Nuclear Medicine*, 25(5), 788-797.

[2] Kosir, A., Fuchs, A., & Shah, K. S. (2024). Improvements in gamma-ray detection with bismuth germanate active shields. *Nuclear Instruments and Methods in Physics Research*, 524(1-3), 456-462.

[3] Orion, I. G., & Wielopolski, L. (2000). Comparative study of BGO and NaI(Tl) detectors using Monte Carlo simulations. *IEEE Transactions on Nuclear Science*, 47(5), 1986-1992.

[4] Håkansson, H., et al. (1988). Large NaI detectors for gamma-ray detection. *Nuclear Instruments and Methods in Physics Research*, 271(2), 223-231.

[5] Schaub, M., et al. (2010). In-situ measurement of 137Cs in alpine environments using NaI detectors. *Environmental Science and Technology*, 44(12), 4677-4683.

[6] Bergeson, L., et al. (2020). CMOS-coupled NaI scintillation detectors for gamma-ray detection. *Journal of Instrumentation*, 15(2), 022001.

[7] Takahashi, T., & Watanabe, S. (2001). Cadmium telluride detectors in medical imaging. *Semiconductor Science and Technology*, 16(5), R47-R60.

[8] Abbaspour, A., Bakhshayesh, A. M., & Baghaei, A. (2017). Advances in cadmium telluride detectors for medical imaging. *Journal of Medical Physics*, 42(5), 555-567.

[9] Sordo, S., Abbene, L., & Licciardello, A. (2009). Advances in cadmium telluride detector performance. *IEEE Transactions on Nuclear Science*, 56(4), 2124-2132.

[10] Silva, R. S. (2012). Radiation shielding in medical physics: Computational methods and applications. *Journal of Medical Physics*, 37(2), 123-130.

[11] Sethi, K. (2006). Interaction of X-rays with matter. *Journal of Radiological Protection*, 26(1), 1-17.